Transport properties of highly doped polycrystalline and amorphous SnO_2 films

Didier Jousse*
Instituto de Fisica, Unicamp Caixa Postale 6165, 13100 Campinas, São Paulo, Brazil
(Received 7 December 1983; revised manuscript received 25 September 1984)

The Hall effect in the temperature range 80—500 K has been measured in sprayed SnO_2 films deposited at low substrate temperatures, $220 \leq T_s \leq 440$ °C. The data indicate the classical behavior of degenerate semiconductors for polycrystalline films prepared at $T_s \geq 350$ °C. With the lowering of T_s, the conduction ceases to be metallic either due to the incorporation of excess Cl donor impurities or the appearance of the amorphous state when $T_s < 300$ °C. We interpret the Hall-effect data by a generalized two-band model where a fraction of the electronic states remains strongly localized. Quantitative estimates are given for two types of disorder: a distribution of Cl impurity atoms in a polycrystalline matrix, and an amorphous host-lattice structure. The mobility of amorphous SnO_2 was measured down to 80 K and the values between 0.4 (80 K) and 1.5 $cm^2 V^{-1} s^{-1}$ (500 K) are compatible with electron transport via extended states in both the conduction-band and impurity-band regimes.

I. INTRODUCTION

Sprayed SnO_2 films are commonly used as antireflecting coatings or as surface barriers in photovoltaic devices because of their high electrical conductivity, combined with their low absorption in the visible spectrum. Many experimental findings have been reported on the electrical and optical properties of undoped or doped films[1] generally prepared at substrate temperatures T_s higher than 400 °C. On the other hand, very little is known of the physical properties of SnO_2 at low T_s.

The sprayed films are amorphous when prepared at substrate temperatures lower than 300 °C.[2] The recent results of secondary-ion-emission—spectroscopy (SIMS) and Auger-electron—spectroscopy (AES) analysis by Chambouleyron *et al.*[3] have revealed that chlorine atoms are always present in the films and that their concentration varies strongly with T_s from 10^{-4} ($T_s = 490$ °C) to a few atomic percent ($T_s = 260$ °C). The high conductivities measured in both polycrystalline and amorphous films deposited at low T_s (Ref. 4) may be related to nonintentional chlorine doping and not to oxygen vacancies as in chemical-vapor-deposited (CVD), pure single crystals.[5]

Intentional *n*-type doping has been achieved for the first time for substitutional Sb (tin sites) and F (oxygen sites).[6] Many results are available in the literature from studies of films doped with well-controlled doping ratios of Sb,[7,8] F,[9] or group-III elements such as In or Tl.[10] The conductivity is shown to increase with doping ratio up to 10^3—10^4 $\Omega^{-1} cm^{-1}$ for a concentration of a few mol % in the spray solution. In general, large additions of dopants produce a reduction of the charge-carrier concentration for a doping ratio higher than 5 mol %. At the same time, the Hall electron concentration and mobility become temperature dependent. This metal-nonmetal transition was first observed by Inagaki *et al.*,[7] and it has been suggested that the reduction in charge-carrier concentration may be related to increased disorder.[10]

The present paper deals mainly with Hall-effect measurements in the temperature range 80—500 K on polycrystalline and amorphous SnO_2 films prepared by the spray technique at low T_s. One purpose of it is to analyze the transport properties of SnO_2 films in the presence of a high concentration of Cl doping atoms and/or disorder. We also analyze the optical-absorption data obtained on such films. The shrinking of the optical gap suggests the emergence of a band associated with Cl impurities. A model is proposed for the interpretation of the Hall-effect data on the very highly doped polycrystalline and amorphous samples. Electronic conduction is assumed to take place in impurity- and conduction-band states. The classical two-band model is modified to take into account the localization of a fraction of the electronic states. The fit to the experimental results supports this interpretation, but leaves open some questions concerning the nature of transport in the bands.

II. EXPERIMENTAL DETAILS

SnO_2 films nearly 0.5 μm thick were deposited on glass substrates by spraying an alcohol solution of stannic chloride. Details of this experimental setup have been described elsewhere.[2,3] X-ray-diffraction patterns obtained with a 12-kW Rigaku Rotaflex rotating-anode diffractometer were used to detect the amorphous nature of the films or the grain size of polycrystalline films. The electrical conductivity and the Hall coefficient were measured by the van der Pauw technique on samples measuring 7 mm × 7 mm. Ohmic contacts were obtained by a metalized epoxy baked at 150 °C. All measurements were made with a current of 100 μA and in a magnetic field B in the range 5—20 kG. Opposite directions of sample current and magnetic field were taken to eliminate thermal and contact effects. In view of the low values of the Hall voltage ΔV_H, the Hall coefficient R_H at each measurement temperature was deduced from the plot of ΔV_H as a function of B, which appears linear up to 20 kG. The final uncertainty on R_H was between 5% and

10%, except for the amorphous samples above room temperature, where it reached 20%. The conductivity was measured to an accuracy of 2% and we did not observe any magnetoresistance effect at the highest applied magnetic field. Sprayed SnO_2 films are known to be very sensitive to annealing. We therefore verified, after the measuring process from 80 to 500 K, that the electrical parameters returned to their initial room-temperature values.

III. PHYSICAL CHARACTERIZATION

X-ray diffraction shows the absence of crystallinity for samples prepared below 300 °C. On samples prepared above 300 °C, a diffraction pattern is observed with the main peak in the [200] direction, which indicates a preferential orientation of the grains with the c axis parallel to the substrate. Application of Scherrer's formula to this peak gives a grain size between 200 and 500 Å, slightly increasing with T_s.

The Hall coefficients of all samples were negative, even in the amorphous ones. The classical Hall treatment is expected to apply when the mean free path remains of the order or is larger than the mean distance between scattering centers.[11] The high mobility values we obtain are consistent with the classical regime. The electron Hall concentrations can thus be deduced from the classical formula $R_H = -1/qn_H$, assuming a scattering Hall coefficient equal to unity. This last assumption is strictly valid in the case of a degenerate electron gas, and is within our measurement uncertainties for the nondegenerate case.

We shall consider first the room-temperature values of n_H for samples prepared between 220 and 520 °C. The results are plotted in Fig. 1 as a function of inverse substrate temperature, together with chlorine contents [Cl] deduced from SIMS and AES compositional analyses.[3] The mechanism of chlorine doping at low T_s appears rather complicated, but we can distinguish the following three classes of materials according to the substrate temperature and the doping efficiency defined as $\eta = n_H/[\mathrm{Cl}]$.

(i) Class I: $350 \leq T_s \leq 500$ °C, polycrystalline, $[\mathrm{Cl}] = 10^{-2}$ at. %, $\eta \sim 100\%$. In this range, all Cl atoms introduced in the lattice behave as active donors.

(ii) Class II: $300 \leq T_s < 350$ °C, polycrystalline, $[\mathrm{Cl}] = 10^{-1}$–1 at. %, η is a decreasing function of T_s down to $\eta \sim 10\%$ ($T_s = 300$ °C). The losses in doping efficiency may have various origins: segregation at grain boundaries or clustering of Cl atoms, compensation effect by creation of acceptor states, or lattice disorder induced by dopants.

(iii) Class III: $T_s < 300$ °C, amorphous, $[\mathrm{Cl}] > 1$ at. %, $\eta \sim 0.1$–1 %. Such a low doping efficiency is common to many doped amorphous semiconductors.

At substrate temperatures higher than 500 °C, alkali ions from the glass substrate diffuse into the film,[1] leading to compensation of the chlorine doping. At the other end of the temperature range, the hydrolysis reaction no longer occurs (below 150 °C). Conductive amorphous SnO_2 is thus obtained in a narrow range, between 280 and 180 °C. There is appreciable scatter in the Hall data, as shown in Fig. 1 for $T_s = 220$ °C, presumably associated with the sluggishness of the low-temperature reaction.

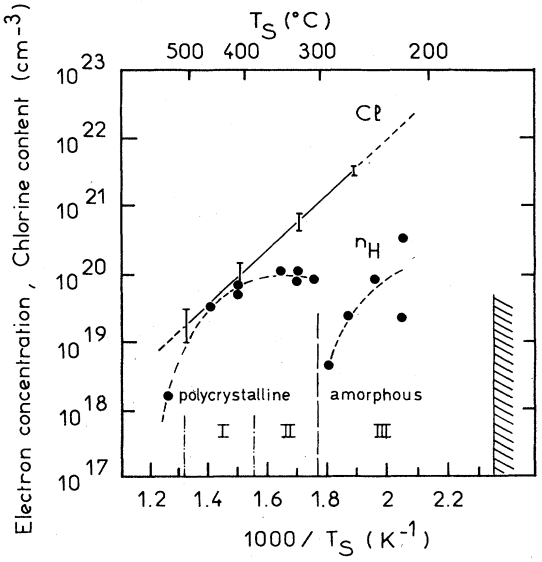

FIG. 1. Hall-electron concentration at 300 K and chlorine content (from Ref. 3) plotted as a function of inverse substrate temperature.

Conductivity and Hall-effect measurements as a function of temperature have been performed on samples representative of each one of the previously defined classes of materials. For this purpose, samples with the best voltage signal-to-noise ratios at the contacts have been selected. They are labeled by the letter A or P for amorphous or polycrystalline, followed by the substrate temperature. The results are described in the next section.

Now we would like to comment briefly on the evolution of the optical properties. These have been partly described in a previous paper[2] and we shall recall the main results necessary to better understand the transport properties. The absorption coefficients α versus photon energy $h\nu$ are given in Ref. 2 for samples prepared at 320 and 280 °C ($P320$ and $A280$ using our classification), thus representative of class II and III, respectively. The spectra show two distinct regions: an absorption tail with α rising exponentially with photon energy up to ~3.7 eV, and the fundamental absorption edge at higher energies. In the former region, often known as Urbach tail, α takes higher values upon lowering T_s, which was explained by an increase of the dopant-atom concentration and disorder.[2] We think this is the main reason for a change in aspect of the films: class-I materials are clear, whereas class-II and -III materials are light-brown by transmission.

The absorption edge can be used to determine the optical gap for allowed direct transitions E_g through the relationship $\alpha = \alpha_0(h\nu - E_g)^{1/2}$. In moderately doped SnO_2 polycrystalline films, the linearity of the α^2-versus-$h\nu$ plot has been experimentally verified over a large energy range by a great number of authors,[7,8,12] and the E_g values range between 4.05 and 4.6 eV, depending on the free-carrier concentration (Moss-Burstein shift). On the other hand, if we take the α values of Ref. 2 for samples $P320$ and $A280$, we obtain linear portions of the α^2-versus-$h\nu$

plots in a very small energy range, the extrapolated E_g values being 3.93 and 3.89 eV, respectively. A better fit is obtained if we plot the same data in the form $(\alpha h\nu)^{1/2}$ versus $h\nu$ as shown in Fig. 2. A law of the type $\alpha h\nu = B(h\nu - E_0)^2$ is experimentally verified in most amorphous semiconductors and is expected theoretically in two cases:[11] (i) extended- to extended-state transitions dominate, and the densities of states beyond the mobility edges in both the valence and conduction band are parabolic. In this case, $E_0 = E_c - E_v$; (ii) extended- to localized-state transitions dominate and the density of localized states in the band tail varies linearly with energy. Then, E_0 is the energy distance between a mobility edge and the edge of the band tail: $E_0 = E_c - E_v - \Delta E$, where ΔE is the width of the band tail. The B values of 1.2×10^5 and 1.8×10^5 $cm^{-1}eV^{-1}$ for samples $P320$ and $A280$ are in agreement with the predicted values of the second model with $\Delta E \sim 0.2$ eV. However, without a precise knowledge of the form of $g(E)$ at the band edges, no definite interpretation can be given. The extrapolated E_0 values of 3.4 ($P320$) and 3.2 eV ($A280$) are well below the usual gap of polycrystalline SnO_2 films.

The general features in optical properties as one goes from class-I to class-II and -III materials are thus an increase in the exponential absorption tail and a shift of the absorption edge to lower energies. A modification of the electronic structure including the existence of band tails of localized states must be considered in class-II and -III materials.

IV. CONDUCTIVITY AND HALL EFFECT AS A FUNCTION OF TEMPERATURE

The conductivities versus reciprocal temperature of four SnO_2 samples are given in Fig. 3. The nearly-temperature-independent conductivity of polycrystalline SnO_2 indicates, at first, that the Fermi level E_F lies above

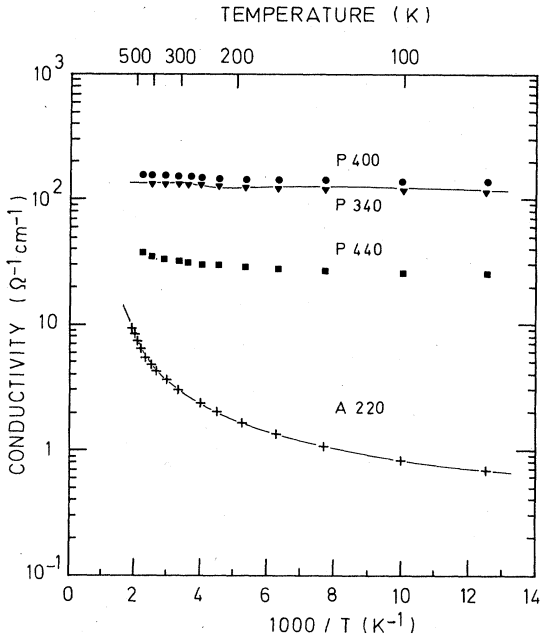

FIG. 3. Variations of the conductivity as a function of reciprocal temperature of polycrystalline and amorphous SnO_2 films. The theoretical curves for samples $A220$ and $P340$ (solid lines) have been obtained from the fitting with the generalized two-band model (see text).

E_C. It suggests that the impurity band formed by the Cl donor states has merged into the conduction band in this range of Cl concentration. On the other hand, two distinct regimes are observed for the amorphous $A220$ films: a well-defined activated regime above 400 K and a low-temperature regime which cannot be defined by a single activation energy. The first regime is associated with the transport of electrons excited above the mobility edge E_C, and the activation energy of 0.11 eV should correspond to

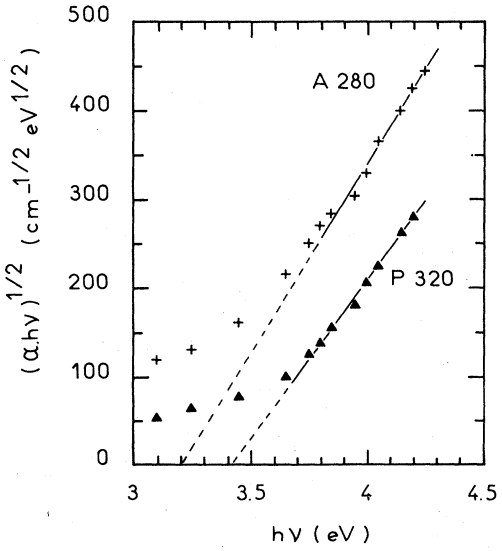

FIG. 2. $(\alpha h\nu)^{1/2}$-vs-$h\nu$ plots for SnO_2 films prepared at 320 and 280 °C using the data of Ref. 2.

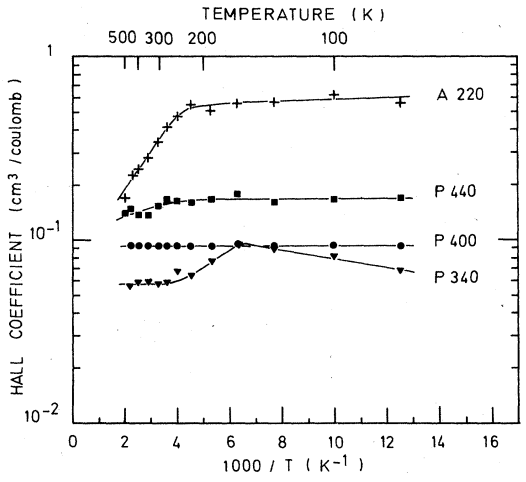

FIG. 4. Temperature dependence of the Hall coefficient of polycrystalline and amorphous SnO_2 films from 80 to 500 K.

$E_C - E_F$, assuming a constant mobility as a function of temperature. This assumption is not valid, as we will show. At low temperature we observe a gradual change in slope from 0.11 eV to values of the order of 10^{-2} eV, which cannot be understood on the basis of the classical theory for impurity-band conduction.[13,14] The knowledge of the carrier concentration and mobility in this region is essential in order to clarify the nature of transport in amorphous SnO_2.

The Hall coefficients R_H versus reciprocal temperature are shown in Fig. 4 for the four samples of Fig. 3. The Hall mobilities $\mu_H = |R_H|\sigma$ for the same samples are shown as a function of temperature in Fig. 5. The analysis of R_H and μ_H curves will be taken up in Sec. V after a brief discussion of the theoretical predictions of the two-band model and the occurrence of metallic conduction.

V. RESULTS, ANALYSIS, AND DISCUSSION

A. Theoretical predictions

1. Metallic conduction and impurity-band conduction

The concept of impurity-band formation due to the interaction between impurity states was first successfully used by Hung and Gliessman,[15,16] and Fritzsche,[13] to interpret their results on Ge. The theory of impurity conduction was reviewed by Mott and Twose,[14] with special emphasis on the critical concentration N_C of donors N_D (n-type material) at which the transition to the metallic conductivity occurs. For quantitative analysis of N_C, one assumes the hydrogenic nature of the donors, and must compare the average interdonor distance $d=(3/4\pi N_D)^{1/3}$ with their effective Bohr radius $a_0=0.53(m/m^*)(\epsilon/\epsilon_0)$ Å, where ϵ is the dielectric constant, m the free-electron mass, and m^* the electron effective mass. According to the Mott criterion,[17] metallic conductivity takes place when $d/a_0 < 2.5$. Data on the ratios ϵ/ϵ_0 and m/m^* for SnO_2 films are scarce, but are sufficient for a rough estimate of a_0. For F-doped films Skornyakov and Surkova[9] gave a value of $m^*=0.2$ when the electron concentration is lower than 10^{20} cm^{-3}. Shanthi *et al.*,[8] in their study of undoped and Sb-doped films, deduced that $m^*=0.1m$ for the same electron concentration. We shall use, for our estimate, the mean value $m^*=0.15m$. The values of the dielectric constant have been reported by Van Daal[18] for single-crystal SnO_2: $\epsilon_{\|}=9$ and $\epsilon_{\perp}=14$ in the directions parallel and orthogonal to the c axis, respectively. We shall admit, in a first approximation, an effective dielectric constant for our films: $\epsilon_r=\epsilon/\epsilon_0=(\epsilon_{\|}\epsilon_{\perp}^2)^{1/3}\simeq 12$. From these values, we deduce that $a_0\simeq 42$ Å. The estimation of N_D cannot be made from the chemical analysis of the films because we suspect that preferential segregation of Cl atoms takes place at grain boundaries in polycrystalline films. In the same way, in amorphous films, a portion of Cl atoms may be involved in configurations where they do not act as donor centers. We prefer to take a lower limit of N_D from the high-temperature part of the R_H curves. If N_A is the concentration of acceptor states simultaneously present in the samples, the exhaustion concentration of electrons is $n_0=N_D-N_A=1/qR_{H\,\mathrm{exh}}$, and n_0 can be taken as a lower limit of N_D. We obtain, for our samples, a ratio $d/a_0 < 0.5$, which indicates clearly that our donor concentration is well above the metallic concentration.

The experimental results agree with this prediction only for class-I materials. In fact, the Mott criterion cannot be applied to class-II and -III samples, which must be considered disordered alloys due to the high Cl concentration. The impurities can no longer be assumed to lie on a regular lattice of the host atoms, and the hydrogenic model becomes incorrect.[19] In the presence of disorder, the ionization energies associated with the Cl impurities lead to a

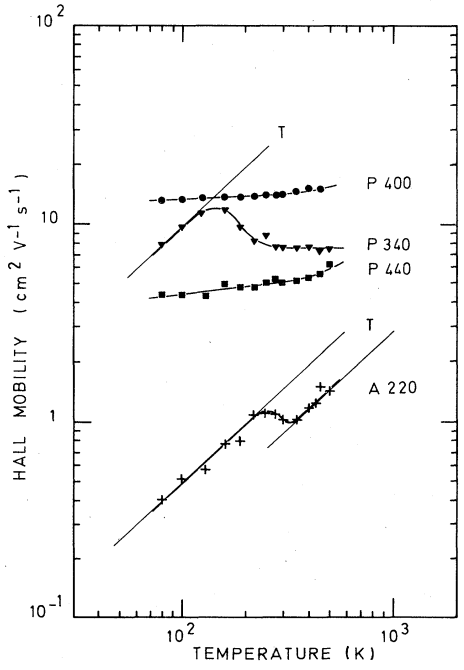

FIG. 5. Temperature dependence of the Hall mobility for the samples of Fig. 2.

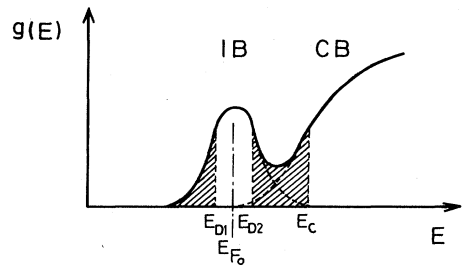

FIG. 6. Schematic representation of the density-of-states distribution for electrons in SnO_2:Cl considered as a disordered alloy. IB and CB denote impurity band and conduction band, respectively. E_{D1}, E_{D2}, and E_C denote mobility edges demarcating extended states from localized states (shown hatched).

broadened impurity band. A localization of the Anderson type[20] may occur for states whose energy is too distant from the centroid of the distribution. We think that this is the case for amorphous SnO_2:Cl. A schematic representation of the density-of-states distribution $g(E)$ is given in Fig. 6, where we assume that impurity- and conduction-band states are distinguishable and separated by a mobility gap. The variations of the R_H curve for the amorphous sample $A220$ in Fig. 4 indicate that electrons are in an impurity band below 250 K, and, above that temperature, are excited at a conduction-band mobility edge. The question arises as to whether this picture also described properly the $g(E)$ distribution of polycrystalline SnO_2:Cl at high doping levels. Some arguments are given in Sec. V B 2. We note in Fig. 4 that the R_H curve of sample $P340$ presents a conspicuous maximum around 180 K which is characteristic of a transition between conduction- and impurity-band conduction.

Before going further in the discussion, we summarize in the following section the theoretical results expected on the basis of the two-band model, taking into account, at the same time, the localization of a fraction of the electronic states.

2. Generalized two-band model

We call n_C,μ_C the number of carriers and the microscopic mobility in the conduction band, and n_D,μ_D the same quantities for the impurity band. Following the arguments of the preceding subsection, we consider that a finite number of electrons occupy localized states (concentration n_L). These states are trapping centers, i.e., the associated mobility is taken to be equal to zero. Their main effect is on the concentrations n_C and n_D, the total number of electrons being given by

$$n=n_C+n_D+n_L \ , \tag{1}$$

which is a known quantity in the exhaustion regime $n_0=N_D-N_A$. The classical relations for the conductivity, Hall coefficient, and Hall mobility[16] still apply. For the sake of simplicity, we shall assume in the following, as in most studies based on the two-band model, that Hall mobilities are equal to the microscopic mobilities in the two bands. We have the following expressions:

$$\sigma=q(n_C\mu_C+n_D\mu_D) \ , \tag{2}$$

$$R_H=\frac{\mu_C^2 n_C+\mu_D^2 n_D}{q(\mu_C n_C+\mu_D n_D)^2} \ , \tag{3}$$

$$\mu_H=\frac{\mu_C^2 n_C+\mu_D^2 n_D}{\mu_C n_C+\mu_D n_D} \ . \tag{4}$$

The determination of the quantities μ_C, n_C, μ_D, and n_D can be made through the low- and high-temperature limiting cases.

The main difference between Eqs. (1)—(4) and the classical two-band model is that the low-temperature plateau of the R_H curve is higher than the exhaustion value $R_{H\,\mathrm{exh}}$, as the Hall effect will measure only $n_D=N_D-N_A-n_L$.

At the intermediate temperatures, expression (3) presents a maximum which is obtained in the classical two-band model when $n_C\mu_C=n_D\mu_D$ and the general shape of the R_H curve is a symmetrical peak separating two plateau regions. This is no longer the case when the concentration n_L is introduced in the calculations, as shown in the application of the model.

B. Results, analysis, and discussion

We shall first discuss the experimental results of polycrystalline films with the distinction between class-I and -II materials. In particular, we shall take into account the effect of grain boundaries on the measured Hall effect. Then, we shall analyze more extensively the results of amorphous films.

1. Class-I polycrystalline films (P440, P400)

The interpretation of conductivity and Hall-effect results on polycrystalline materials has been reviewed recently by Orton and Powell.[21] In general, trapped interface charges at the grain boundaries lead to intergrain band bending and potential barriers. In view of our doping levels, the depletion region extends to only a few angstroms; that is, much less than the grain diameter. Hence, the Hall effect measures the true carrier concentration in the bulk of the grain, while one would expect the Hall mobility to be given by the Petriz formula for grain-boundary scattering:[22]

$$\mu_G=AT^{-1/2}\exp(-q\phi_b/kT) \ , \tag{5}$$

where ϕ_b is the potential-barrier height and A is related to the grain diameter. The contribution of grain-boundary scattering to mobility is added to the other scattering mechanisms using Mathiessen's rule. Following the arguments of Shanthi *et al.*,[8] we can neglect, in SnO_2 films, acoustic and optical lattice scattering. The Hall mobility is then given by

$$1/\mu_H=1/\mu_G+1/\mu_I \ , \tag{6}$$

where μ_I is the mobility for ionized-impurity scattering. An analytic expression has been given by Mott[23] for a degenerate gas, and according to Mansfield,[24] may be written as

$$\mu_I=1.27\times10^{-7}(\epsilon/\epsilon_0)^2(m/m^*)^2\frac{n}{N_I f(x)} \ , \tag{7}$$

with

$$f(x)=\ln(1+x)-x/(1+x)$$

and

$$x=(4.1\times10^{-11})(\epsilon/\epsilon_0)(m/m^*)n^{1/3} \ ,$$

where n and N_I denote concentrations of free electrons and charged centers, respectively. Assuming that donors and acceptors are totally ionized and that each one contributes one single charge, the ration n/N_I may also be written in the exhaustion regime as $(1-K)/(1+K)$, where K is the compensation ratio $K=N_A/N_D$. Taking, for n, the exhaustion values of n_0 from Fig. 4, and $K=0$, $\epsilon/\epsilon_0=12$, and $m^*=0.15m$, we obtain, for samples $P440$ and $P400$,

$\mu_I = 16.6$ and 29.7 $cm^2 V^{-1} s^{-1}$, respectively, independent of temperature. These values are a few times higher than the measured μ_H, but of the order of the highest reported values in SnO_2 films.[25] The observed increase of mobility with temperature comes from the contribution of grain-boundary scattering, and a good fit is obtained above 250 K using the above μ_I values and relations (5) and (6), leading to the following values of the parameters: $A = 240$ $cm^2 V^{-1} s^{-1} K^{1/2}$, $\phi_b = 0.025$ eV and $A = 10^3$ $cm^2 V^{-1} s^{-1} K^{1/2}$, $\phi_b = 0.019$ eV for samples *P*440 and *P*400, respectively. At lower temperatures, tunneling of electrons through the intergrain barriers is responsible for the temperature-independent mobility. Thus we conclude that grain-boundary scattering is the main scattering mechanism in polycrystalline SnO_2:Cl films deposited at high substrate temperature, as was previously shown in undoped films.[8]

2. *Class-II polycrystalline film (P340)*

We have attempted unsuccessfully to interpret the experimental curves with the classical theory for one type of carrier. One could argue that the variations of the electron concentration $n_H = -1/qR_H$ are due to the displacement of the Fermi level within the perturbed conduction band. The temperature independence of μ_H above 300 K indicates that grain-boundary scattering does not limit the mobility of free electrons. Thus, we have attempted to fit the μ_H curve considering pure ionized-impurity scattering. The compensation ratio was adjusted for the high-temperature region using relation (7). With the above values for ϵ/ϵ_0 and m^*, K is equal to 0.53. The theoretical curve for μ_I [dashed line of Fig. 7(b)] is obtained using relation (7) and the n values from the experimental Hall-coefficient curve. The variations of μ_I are too smooth to fit the experimental data.

To treat the model with two types of carriers, we have seen, in Sec. V A, that conduction- and impurity-band states must be considered distinguishable. It would mean that, after merging into the conduction band above a critical Cl concentration N_C, the impurity band is driven out of the conduction band when [Cl] exceeds another limit concentration. There is some evidence for this behavior of SnO_2 films from the study of Rohatgi *et al.*,[10] who have intentionally introduced group-III (In,Tl) and -V (Sb,P) dopants. The charge-carrier concentrations reach a maxima for nearly 3 mol % doping in the solution, and the activation energies of the conductivity drop to 0.0015 eV (Sb and P doping) and 0.0175 eV (In and Tl doping). Further additions of dopants up to 30 mol % lead to an increase of the activation energy to 0.06 and 0.07 eV, respectively. X-ray diffraction revealed that the addition of In and Sb caused large changes in crystallographic orientations, whereas additions of Tl and P increased disorder. This means that E_F has been shifted below a conduction-band mobility edge as a consequence of disorder. In the same way, as shown in Fig. 7(a), a well-defined activation energy is obtained for the electron concentration of sample *P*340 in the high-temperature region. X-ray-diffraction measurements on our films do not show any alteration of the crystallographic orientations as the substrate temperature decreases, but only a broadening of the main diffraction peak corresponding to the [200] orientation.

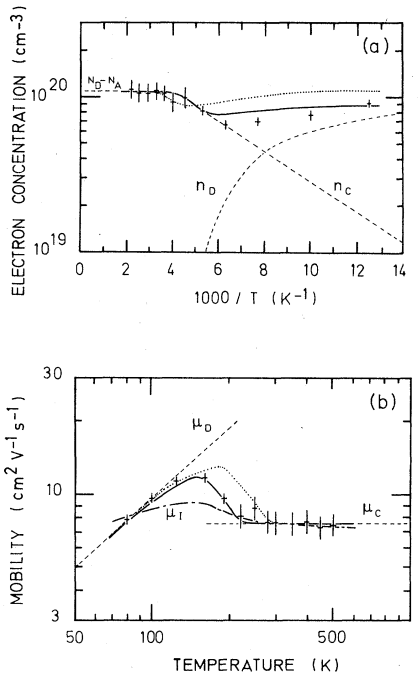

FIG. 7. Theoretical curves of (a) Hall-electron concentration and (b) Hall mobility for sample *P*340 using the usual (dotted line) and generalized (solid line) two-band models. For the last case, the variations of n_C, n_D, μ_C, and μ_D used for the fitting are indicated by dashed lines. Also represented in (b) are the variations of μ_I expected from the classical one-carrier model.

For the fit with the modified two-band model, we shall determine the quantities μ_C, n_C and μ_D, n_D from the high- and low-temperature regions, respectively, of the μ_H and R_H curves. n_C is obtained by extrapolation of the $1/qR_H$ values in the high-temperature range, and we take, for μ_C, a constant value of 7.7 $cm^2 V^{-1} s^{-1}$.[26] In the temperature range 80–160 K, the electrons are mainly in the impurity band and their number n_D is given by relation (1). We take, for $N_D - N_A$, the exhaustion value $n_0 = 1.07 \times 10^{20}$ cm^{-3}, and n_L is taken to be an adjustable parameter. The states of concentration n_L are strongly localized and we consider that the electrons will freeze first on these centers, and only at the lowest temperatures in the delocalized ones of concentration n_D. From the μ_H curve we assume a linear variation of μ_D with temperature, $\mu_D = 0.1T$ [dashed line of Fig. 7(b)]. The theoretical curves for R_H and μ_H in Figs. 7(a) and 7(b) have been obtained with two values of n_L: 0 (classical two-band model) and 1.8×10^{19} cm^{-3} (generalized two-band model). These values clearly show the effect of the localization of a part of the donor states which introduces a strong asymmetry in the n_H curve. The experimental points are represented with their attached uncertainties. The best simultaneous fitting of the two curves has been obtained with $n_L = 1.8 \times 10^{19}$ cm^{-3}, which is 17% of the exhaustion value. Finally, the fitting is better with a constant μ_C value than it is with μ_C taken as μ_I and varying with n_C, according to (7) [dotted line of Fig. 7(b)].

3. *Amorphous SnO_2 film (A220)*

The amorphous films remain transparent in the range 0.6—1.1 μm, which indicates that the density of states is low in the forbidden gap.[4] This is consistent with the possibility of Cl doping, because there is no strong pinning of the Fermi level by midgap states. However, the large Urbach tail of absorption and the shift of the absorption edge toward small energies suggest the existence of a broad tail of states in the vicinity of the mobility edge E_C in the way sketched in Fig. 6.

The R_H curve of Fig. 4 clearly shows that electrons are mainly in an impurity band at low temperature and are progressively excited in the conduction band at temperatures higher than 250 K. As the Fermi level lies well beneath the mobility edge E_C, the concentration of electrons in the conduction band is given in the Boltzmann approximation by

$$n_C = \mathcal{N}_C \exp\left[-\frac{E_C - E_F}{kT}\right],$$

where $\mathcal{N}_C$ is the effective density of conduction-band states.

Both mobilities μ_C and μ_D increase linearly with temperature (Fig. 5), and their variations are well described by the following laws: $\mu_C = (2.9\times10^{-3})T$ and $\mu_D = (4.9\times10^{-3})T$. The transition between the two regimes occurs at around 250 K, when the population of electrons begins to predominate in the conduction band. The quantity $N_D - N_A$ is unknown, and we are unable to deduce n_D from relation (1). We have proceeded in the following way for the fitting of the experimental data: $\mathcal{N}_C$ and $E_C - E_F$ are taken as adjustable parameters, and the concentration n_D is an adjustable function of temperature. In fact, n_D does not vary in a simple way because of the presence of the large quantity of localized states, n_L. The decrease of μ_H between 220 and 350 K is explainable only if n_D decreases rapidly with increasing temperature, although remaining of the order of n_C. Thus we introduced, in an *ad hoc* fashion, the following T dependence of n_D:

$$n_D = (1.1\times10^{19})[1+\exp(T-T_0)/\Delta T]^{-1}.$$

This expression does not have a clear physical meaning. The reasons we may invoke for the rapid decrease of n_D as T increases above 220 K would be rather speculative at the present stage of study. Thermoelectric-power measurements are necessary to obtain valuable information on the structure in $g(E)$ or a possible shift of E_F with temperature. We again assume that electrons primarily fill the trapping centers and, very progressively, the proper donor band states. The theoretical curves of Figs. 8(a) and 8(b) have been obtained with use of the following parameters: $\mathcal{N}_C = 1.8\times10^{20}$ cm^{-3}, $E_C - E_F = 0.07$ eV, $T_0 = 280$ K, and $\Delta T = 60$ K. As uncertainties on R_H and μ_H are large, we ensured that the theoretical μ_H/R_H curve fits the $\sigma(T)$ curve with a 4% margin of error (solid line in Fig. 3). We have also illustrated, in Fig. 8(a), the variations of n_C and n_D (dashed lines) and what the concentration n_L deduced from (1) with an arbitrary value $N_D - N_A = 5\times10^{19}$ cm^{-3} would be. The comparison between n_D and n_L at low temperature indicates that 80% of the electrons are on localized states, which is the inverse of sample $P340$. The fit of the theoretical R_H and μ_H curves with the experimental data is excellent in view of the simplicity of the analytical functions used for the parameters, especially the rough estimate of n_D.

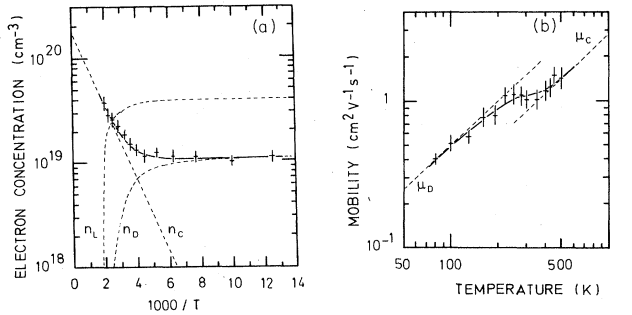

FIG. 8. Theoretical curves of (a) Hall-electron concentration and (b) Hall mobility for sample $A220$ obtained with the generalized two-band model. Indicated by dashed lines are the variations of n_C, μ_C, n_D, μ_D, and also n_L for an arbitrary exhaustion concentration $N_D - N_A = 5\times10^{19}$ cm^{-3}.

4. *Discussion*

A fundamental question is on the nature of conduction mechanisms in both bands. To acquire insight into the problem, we have made ac-conductivity measurements on both $P340$ and $A220$ samples in the frequency range $1-10^5$ Hz. Frequency-dependent conductivity is expected when predominant transport is by hopping carriers between donor states or in the presence of structural inhomogeneities. In our samples, the conductivity does not vary with frequency either at 300 or 80 K. This results rules out our primary suggestion[4] that class-II materials could be composed of both polycrystalline and amorphous phases. Thus, the material can be treated as an homogeneous medium, as is assumed in the two-band model.

On one hand, the frequency-independent conductivity and the mobility values measured at low temperature indicate that electrons are not transported by an hopping process between charged centers of the impurity band. On the other hand, the scattering of electrons in amorphous SnO_2:Cl cannot be described by the theoretical approaches on diffusive carrier motion in the random-phase model, which predicts a T^{-1} dependence.[27—29]

A linear T dependence of the mobility suggests a scattering of electrons by an array of ionized impurities. For the nondegenerate case, a $T^{1.5}$ dependence is theoretically expected for μ_I, while a $T^{1-1.5}$ law is experimentally observed for many doped crystalline semiconductors. In an amorphous material, such a mechanism usually does not dominate due to the strong scattering effect of the random potential associated with the disordered lattice. However, the preservation of the correct sign for the Hall coefficient in our case suggests that the mean free path is long compared with the interatomic spacing.

Another striking point is the similar T dependence of the mobility in the impurity- and conduction-band regimes and its convergence to zero as $T \to 0$. This supports

the idea of a unique scattering mechanism for both kinds of carriers.

VI. CONCLUSION

Hall-effect data on sprayed SnO_2 films have been obtained between 80 and 500 K. The results on polycrystalline films deposited at $T_s > 350\,^{\circ}C$ indicate a metallic conductivity. The electron concentration is temperature independent and the observed Hall mobility is attributed to the contribution of grain-boundary scattering and, to a lesser extent, ionized-impurity scattering.

Nonmetallic conduction is observed on polycrystalline and amorphous SnO_2 films deposited at $T_s < 350\,^{\circ}C$, for which the Cl content is about 10^{-1} or 1 at. %, respectively. A high Cl concentration has an effect comparable to other dopants, such as Sb or F, at high doping ratios. Surprisingly, the impurity-band states appear to distinguish themselves again from the conduction-band states. The results have been interpreted by a generalized two-band model, where a part of the electronic states remains localized. The localization is attributed to the nonhomogeneous distribution of the impurities and/or the amorphous structure of the host lattice. Quantitative information on the concentration of localized states has been obtained from the fitting of the experimental data with the model.

The mobility in amorphous SnO_2 has been measured down to 80 K and the values are compatible with electron motion via extended states in both conduction- and impurity-band regimes, although the transport mechanism remains unclear.

ACKNOWLEDGMENTS

The author gratefully acknowledges the warm hospitality of the Physics Institute, Unicamp (São Paulo, Brazil) and of Professor I. Chambouleyron in particular. He also wishes to thank C. Constantino for his assistance in sample preparation and I. Torriani and M. Fantini for help with the x-ray-diffraction measurements. Thanks are due J. Ranninger for a critical reading of the manuscript. This research was supported in part by Companhia Energetica de São Paulo (CESP).

---

*Present address: Laboratoire d'Etude des Properiétés Electroniques de Solides—Laboratoire Propre du au Centre National de la Recherche Scientifique, Boîte Postale 166, 38042, Grenoble-Cedex, France.

[1]See, for example, the following review papers: Z. M. Jarzebski and J. P. Marton, J. Electrochem. Soc. **123**, 199C (1976); **123**, 301C (1976); **123**, 333C (1976); J. L. Vossen, Phys. Thin Films **9**, 1 (1977); J. C. Manifacier, J. P. Fillard, and J. M. Bind, Thin Solid Films **77**, 67 (1981), and references therein.

[2]I. Chambouleyron, C. Constantino, D. Jousse, R. Assumpçao, and R. Brenzikofer, J. Phys. (Paris) Colloq. **42**, C4-1009 (1981).

[3]I. Chambouleyron, C. Constantino, M. Fantini, and M. Farias, Solar Energy Mater. **9**, 127 (1983).

[4]D. Jousse, C. Constantino, and I. Chambouleyron, J. Appl. Phys. **54**, 431 (1983).

[5]S. Samson and C. G. Fonstad, J. Appl. Phys. **44**, 4618 (1973).

[6]A. Y. Kuznetzov, Fiz. Tverd. Tela (Leningrad) **2**, 35 (1960) [Sov. Phys.—Solid State **5**, 167 (1960)].

[7]T. Inagaki, J. Nakamura, and Y. Nishimura, Fujitsu Sci. Tech. J. **5**, 235 (1969).

[8]E. Shanthi, V. Dutta, A. Banerjee, and K. L. Chopra, J. Appl. Phys. **51**, 6243 (1980).

[9]G. P. Skornyakov and J. P. Surkova, Fiz. Tekh. Poluprovdn. **10**, 867 (1975) [Sov. Phys.—Semicond **10**, 1054 (1976)].

[10]A. Rohatgi, T. R. Viverito, and L. H. Slack, J. Am. Ceram. Soc. **57**, 278 (1974).

[11]N. F. Mott and E. A. Davis, *Electronic Processes in Non-Crystalline Materials* (Clarendon, Oxford, 1979), p. 56.

[12]W. Spence, J. Appl. Phys. **38**, 3867 (1967).

[13]H. Fritzsche, Phys. Rev. **79**, 727 (1950).

[14]N. F. Mott and W. D. Twose, Adv. Phys. **10**, 107 (1961).

[15]C. S. Hung, Phys. Rev. **79**, 727 (1950).

[16]C. S. Hung and J. R. Gliessman, Phys. Rev. **96**, 1226 (1954).

[17]N. F. Mott, J. Phys. (Paris) Colloq. **10**, C4-301 (1976).

[18]H. J. Van Daal, J. Appl. Phys. **39**, 4467 (1968).

[19]E. M. Conwell, Phys. Rev. **103**, 51 (1956).

[20]P. W. Anderson, Phys. Rev. **109**, 1492 (1958).

[21]J. W. Orton and M. J. Powell, Rep. Prog. Phys. **43**, 1263 (1980).

[22]R. L. Petriz, Phys. Rev. **104**, 1508 (1956).

[23]N. F. Mott, Proc. Cambridge Philos. Soc. **32**, 281 (1936).

[24]R. Mansfield, Proc. Phys. Soc. London, B **69**, 76 (1956).

[25]This simple calculation shows that ionized-impurity scattering cannot be neglected, as was done in the work of Shanthi *et al.* (Ref. 8). Particularly, the largest values of μ_H usually reported for F-doped polycrystalline SnO_2 films of about 20 $cm^2 V^{-1} s^{-1}$ are very close to the calculated μ_I value, which is the ultimate value one can achieve after total passivation of the intergrain regions. This is especially so in the case of compensated materials, where μ_I is decreased by the amount $(1-K)/(1+K)$.

[26]This last approximation is roughly correct if one considers that μ_C is nearly T independent, as is expected from relation (9). In fact, this relation has been established for scattering by isolated Coulombic centers and describes, only in the first approximation, the actual situation.

[27]M. H. Cohen, J. Non-Cryst. Solids **4**, 391 (1970).

[28]N. K. Hindley, J. Non-Cryst. Solids **5**, 17 (1970).

[29]L. Friedman, J. Non-Cryst. Solids **6**, 329 (1971).